

8<sup>th</sup> International Conference on Photonic Technologies LANE 2014

## Optimization of beam mode for high efficiency laser thermal forming within metallurgical constraints

Stuart P. Edwardson<sup>a,\*</sup>, Jonathan Griffiths<sup>b</sup>, Ghazal Sheikholeslami<sup>a</sup>, Geoff Dearden<sup>a</sup>

<sup>a</sup>University of Liverpool, Laser Group, School of Engineering, Liverpool, L69 3GH, UK

<sup>b</sup>University of Lincoln, Laser and Photonics Engineering Group, School of Engineering, Lincoln, LN6 7TS, UK

---

### Abstract

In the laser forming (LF) process, laser induced temperature distribution within the work-piece is of paramount importance. Through control of process parameters and depending on work-piece geometry, the temperature distribution can be altered to achieve either localized plastic compressive strains or elastic-plastic buckling. Conventionally, three process parameters are manipulated in order to control the temperature distribution within the work-piece; traverse speed, average power and spot size. Additionally, the intensity distribution and geometrical shape of the beam incident on the work-piece surface can be manipulated. The latter has the potential to be useful in maintaining bend angle per pass whilst working within strict metallurgical constraints. In this paper, the effect of beam intensity distribution and geometrical shape on the LF of automotive grade high strength DP 1000 steel sheet is investigated numerically and experimentally, with particular emphasis on optimization for minimal micro-structural transformation.

© 2014 Published by Elsevier B.V. This is an open access article under the CC BY-NC-ND license (<http://creativecommons.org/licenses/by-nc-nd/3.0/>).

Peer-review under responsibility of the Bayerisches Laserzentrum GmbH

*Keywords:* Laser Forming; Laser Bending; DP1000; Advanced High Strength Steels

---

### 1. Introduction

Laser forming is a highly flexible non-contact method for the shaping of metallic components, Edwardson et al (2010). The process typically involves the use of defocused infrared laser radiation to thermally induce stresses in

---

\* Corresponding author. Tel.: +44-151-794-4639 ; fax: +44-151-650-2305 .

E-mail address: [s.p.edwardson@liverpool.ac.uk](mailto:s.p.edwardson@liverpool.ac.uk)

components. Through manipulation of process parameters and depending on workpiece geometry, either localized plastic compressive strains or elastic-plastic buckling can be achieved, producing out of plane bends in either direction (that is, towards or away from the beam) or in-plane shrinkage.

The well established laser forming technique (Griffiths et al (2011), Griffiths et al 2010, Vollertsen et al (2010)) has the potential to be used in the post-processing and correction of distortion of mechanically formed components. For example, a closed loop system could be implemented in which a mechanically formed component is 'tweaked' to within desired tolerances using an iterative approach. Such an approach would profile the component after each application of laser radiation and increment towards the desired geometry.

Advanced high strength steels (AHSS) such as dual phase (DP) steels play a key role in automotive industry. This is due to their unique material properties, allowing for reduced weight and therefore increased fuel efficiency as well as maintaining or indeed improving crash behavior. DP steels consist of a ferritic matrix interspersed with a hard, martensitic phase in the form of islands. Increasing the volume fraction of hard second phases generally increases the strength of the resulting DP steel. Such steels are produced by controlled cooling from the austenite phase (in hot-rolled products) or from the two-phase ferrite plus austenite phase for continuously annealed cold-rolled and hot-dip coated products to transform some austenite to ferrite before a rapid cooling transforms the remaining austenite to martensite. Depending on the composition and process route, hot-rolled steels requiring enhanced capability to resist stretching on a blanked edge (as typically measured by hole expansion capacity) can have a microstructure containing significant quantities of bainite.

A key disadvantage of DP steels is their reduced formability when compared with conventional steels. This reduced formability manifests itself in the form of increased spring back. Neugebauer et al (2009) noted that heat treatment of the DP steel is required in order to achieve formability comparable with that of conventional mild steels. However, if the heat treatment is applied uniformly to the entire sheet, the high strength of the steel is severely compromised or lost altogether. Neugebauer proposed a localized laser heat treatment to improve the formability only in regions where it is required for subsequent, contact based forming. Laser forming has the potential to combine both of the aforementioned processes, overcoming the springback issue whilst minimizing the heat affected zone (HAZ) so as to retain the bulk material properties of the steel.

In this paper an experimental and numerical investigation into the laser forming of DP 1000 steel is presented, with an emphasis on working within strict metallurgical constraints. The effect of laser process parameters and beam mode on the spatial extent of the HAZ has been predicted.

## 2. Experimental

### 2.1. Experimental Set-Up

An experimental study of LF was conducted on graphite coated 50 x 50 x 1.2 mm DP 1000 steel sheet using a 3.5 kW CO<sub>2</sub> TEM00 fast axial flow laser (PRC Laserdyne 890) with a 5-axis CNC beam delivery system, custom written control software and operating at a wavelength of 10.6 μm and in continuous wave mode. The components were edge clamped, as depicted in Fig. 1.

To study the effect of the process on the metallurgical properties of the material, a Vickers micro hardness test with the specification HV 0.1/10 was used to measure the hardness of samples sectioned by water cooled mechanical saw and carefully ground in order to assess the metallurgical effects of laser heating during laser forming. These sections were subsequently mounted in resin and polished to a grain size in the order of microns. After polishing the samples were stored in a dessicator to avoid oxidation.

2.2. Finite Element Model Development

A thermal model of the laser bending of DP1000 steel was developed in COMSOL Multiphysics.

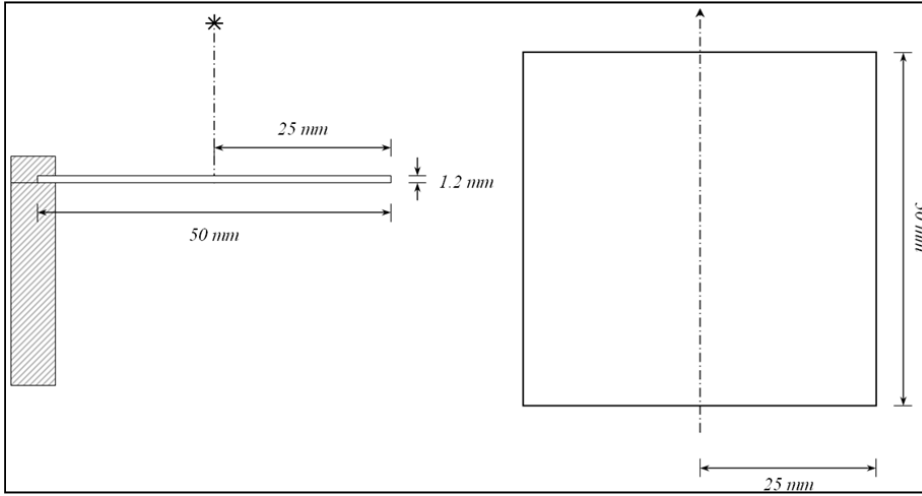


Fig. 1. Schematic diagram of edge clamped cantilever arrangement. Dashed-dot lines represent irradiation path and direction.

The governing equation for conduction in the thermal analysis is:

$$\rho C_p \frac{dT}{dt} = \nabla \cdot (k \nabla T) \tag{1}$$

Where  $\rho$  is the density ( $\text{kg/m}^3$ ),  $C_p$  is the specific heat capacity ( $\text{J/kgK}$ ),  $T$  is the temperature (K),  $t$  is the time (s) and  $k$  is the thermal conductivity ( $\text{W/mK}$ ). The term  $\nabla$  is the differential or gradient operator (sometimes referred to as the Nabla operator) for three dimensional Cartesian co-ordinate systems. All boundaries are subject to convective and radiative heat transfer. Therefore, the heat flux  $q$  at a given boundary is given by:

$$-n \cdot q = -n \cdot (-k \nabla T) = q_0 + h(T_{amb} - T) + \epsilon \sigma (T_{amb}^4 - T^4) \tag{2}$$

Where  $n$  is the normal vector of the boundary,  $h$  is the heat transfer co-efficient ( $\text{W/m}^2\text{K}$ ),  $T_{amb}$  is the ambient temperature (K),  $\epsilon$  is the surface emissivity (1) and  $\sigma_s$  is the Stefan Boltzmann constant ( $\text{W/m}^2\text{K}^4$ ). The intensity distribution  $I$  of the incident laser beam was approximated by a Gaussian distributed heat source:

$$I = I_0 e^{-\left(\frac{2r^2}{\omega_0^2}\right)} = \frac{2P}{\pi r^2} e^{-\left(\frac{2r^2}{\omega_0^2}\right)} \tag{3}$$

Where  $I_0$  is the peak intensity ( $\text{W/m}^2$ ),  $P$  is the average laser power (W),  $r$  is radial distance (m) and  $\omega_0$  is the beam radius (m). Additionally, a flat top intensity distribution ( $I_0 = I$ ) was applied by means of an intensity distribution map generated in MATLAB.

The global mesh element size was set to coarse and determined by a built-in algorithm in COMSOL Multiphysics. A suitable maximum element size for use along the irradiation path was determined by convergence

study and found to be 0.1 mm. The initial thermal output of the model at experimental conditions was verified against thermocouple data before further development, this data is not included here for brevity.

### 3. Results and Discussion

The experimental/numerical work focused on: (i) determination of the effect of laser process parameters on the material properties of DP 1000 (specifically Vickers micro hardness), (ii) thermal simulation of the laser heating process to assess the suitability of process parameter combinations and (iii) thermal simulation to determine the effect of beam mode on the laser heating process.

Initially, the effect of laser process parameters on the micro hardness along the irradiation path throughout the thickness of the component was determined. This was done by varying the traverse speed of the laser whilst keeping the laser power and spot size constant. The centre portion of the steel coupon was sectioned by water cooled mechanical saw and carefully ground in order to assess the metallurgical effects of laser heating during LF. These sections were subsequently mounted in resin and polished to a grain size in the order of microns. Subsequently, Vickers micro hardness measurements were taken at three locations along the irradiation path: 0.15, 0.6 and 1.05 mm from the irradiated surface ( $z = 0$ ). An average of three different measurements at each depth was taken for each sample. The results of this study are shown in Fig. 2.

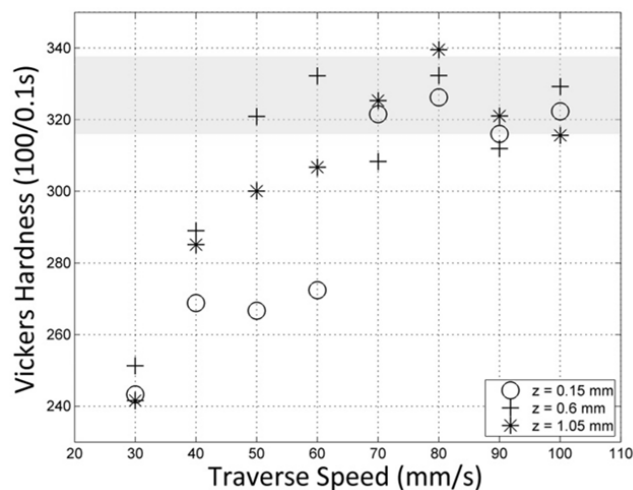


Fig. 2. Vickers micro hardness variation at three reference points with increasing traverse speed, 50 x 50 x 1.2 mm DP 1000, 10 mm beam diameter, 1800 W average power. The shaded band represents the hardness of the steel prior to processing.

Fig. 2 reveals a decrease in measured hardness throughout the thickness of the irradiated area for traverse speeds of less than 60 mm/s, with this effect particularly pronounced with increasing proximity to the surface. For traverse speed greater than 60 mm/s the hardness was comparable to the initial hardness of the steel. To better understand this phenomena a thermal finite element simulation was conducted in which the maximum transient temperature at each of the three reference points was predicted, as shown in Fig. 3.

The slight reduction in hardness observed for traverse speeds above 60 mm/s in Fig. 2 can be rationalised in terms of loss of tetragonality in the martensite upon laser heating. In plain carbon steels, this loss of tetragonality commences at temperatures as low as approximately 370°K and is fully complete at temperatures above approximately 570°K (Bhadeshia et al (2006)). Upon loss of tetragonality, martensite essentially becomes ferrite that is not supersaturated with respect to carbon. As such, the hardness is noticeably reduced. Whilst the presence of additional alloying elements such as Cr, Mo, W, V, Ti and Si have the effect of raising the aforementioned temperatures, the overall effect is the same (Smith et al (2012)).

The relatively larger reduction in hardness observed for traverse speeds below 60 mm/s in Fig. 2 could be attributed to austenitization of the steel during laser heating. As predicted in Fig. 3, these traverse speeds may result in temperatures which are in excess of the upper critical transformation temperature for austenitization. As such, the microstructural composition of the steel after processing would be a function of transformed volume fraction of austenite during heating and subsequent cooling rate. This hypothesis is supported by previous studies, which have shown a limited propensity for martensitic transformation upon cooling for process parameters typical of the laser forming process, Griffiths et al (2011).

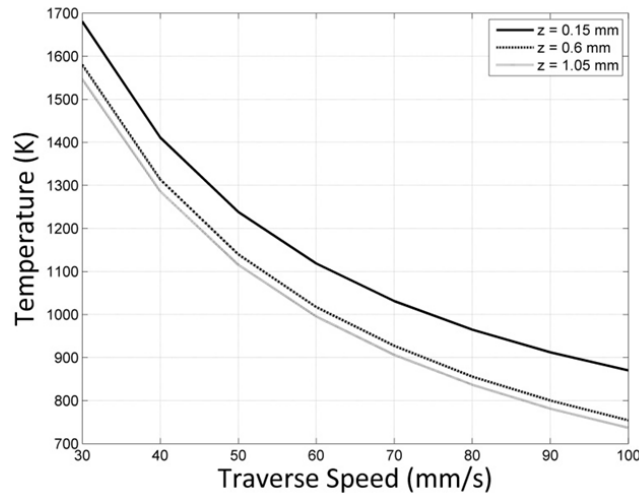


Fig. 3. Simulated peak temperature at three reference points with increasing traverse speed, 50 x 50 x 1.2 mm DP 1000, 10 mm beam diameter, 1800 W average power, 80% absorption.

Given the propensity for micro-structural change during laser heating of DP 1000, it is essential to establish a set of metallurgical constraints to work within to minimise the effect on subsequent material properties such as tensile strength. This can be problematic when manipulating laser parameters to achieve one of the three principle laser forming mechanisms. For example, a uniform temperature profile throughout the sheet thickness may be desired so as to cause in plane shrinkage. The Fourier number  $F_0$  relates laser traverse speed and spot size to the diffusive thermal properties of the material and is a useful quantitative indication of the likely mechanism, Steen et al (2010):

$$F_0 = \frac{\alpha_{th} d_0}{v_0 s_0^2} \quad (4)$$

Where  $d_0$  is the beam diameter,  $v_0$  is the traverse speed and  $s_0$  is the sheet thickness. In order to establish the effect of varying Fourier number on the thermal cycle induced during laser heating of DP 1000, a central parameter set was chosen ( $P = 1800$  W,  $v_0 = 60$  mm/s,  $d_0 = 10$  mm) on the basis of forming efficiency and measured Vickers micro hardness. A simulation was conducted in which the effect of Fourier number on peak temperature and maximum temperature gradient was predicted, as shown in Figure 4. In this case the Fourier number was altered by varying the laser spot size from 5 mm to 15 mm, representative of the transition between the temperature gradient mechanism and bucking or upsetting mechanism.

From Fig. 4 it can be seen that, with increasing Fourier number, the peak temperature is reduced and the temperature gradient diminished. Fig. 5 shows the effect of increasing Fourier number on peak simulated temperature with increasing distance from the irradiation path.

Fig. 5 reveals almost no appreciable variation in simulated peak temperature with increasing distance from the irradiation path with increasing Fourier number, despite significant variation in peak temperature and induced

temperature gradient along the irradiation path. This suggests that the thermal cycle in the irradiation path is of chief importance when assessing the suitability of process parameter combinations with respect to metallurgical constraints.

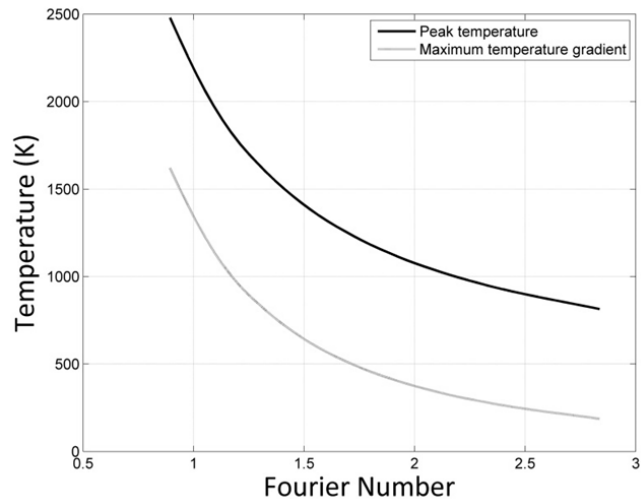


Fig. 4. Simulated peak temperature and maximum temperature gradient with increasing Fourier number, 50 x 50 x 1.2 mm DP 1000, 60 mm/s traverse speed, 1800 W average power, 80% absorption.

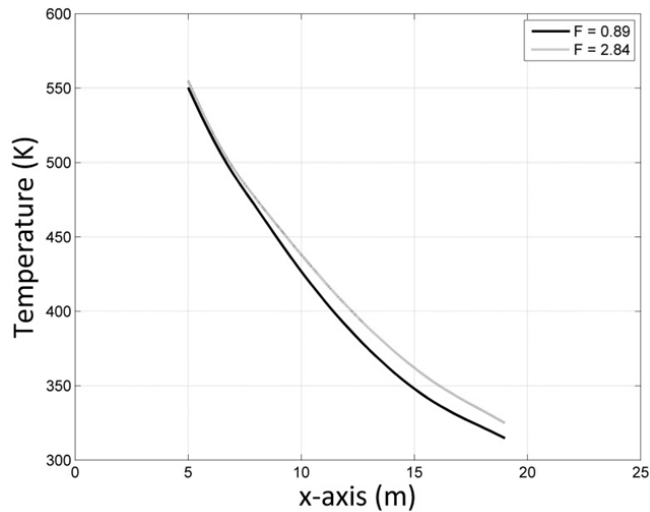


Fig. 5. Simulated peak temperature with increasing distance from the irradiation path, 50 x 50 x 1.2 mm DP 1000, 60 mm/s traverse speed, 1800 W average power, 80% absorption.

Varying the intensity distribution (or beam mode) of the laser beam has the potential to influence the induced thermal cycle in the irradiated region. To establish the magnitude of influence of varying the intensity distribution, two simulations employing the central parameter set ( $P = 1800$  W,  $v_0 = 60$  mm/s,  $d_0 = 10$  mm) were conducted, in

which a Gaussian and flat top intensity distribution were applied. The effect of each on the thermal cycle induced in the irradiated region is shown in Fig. 6.

Fig. 6 shows that the peak temperature and transient temperature gradient are reduced for the flat top intensity distribution relative to the Gaussian intensity distribution.

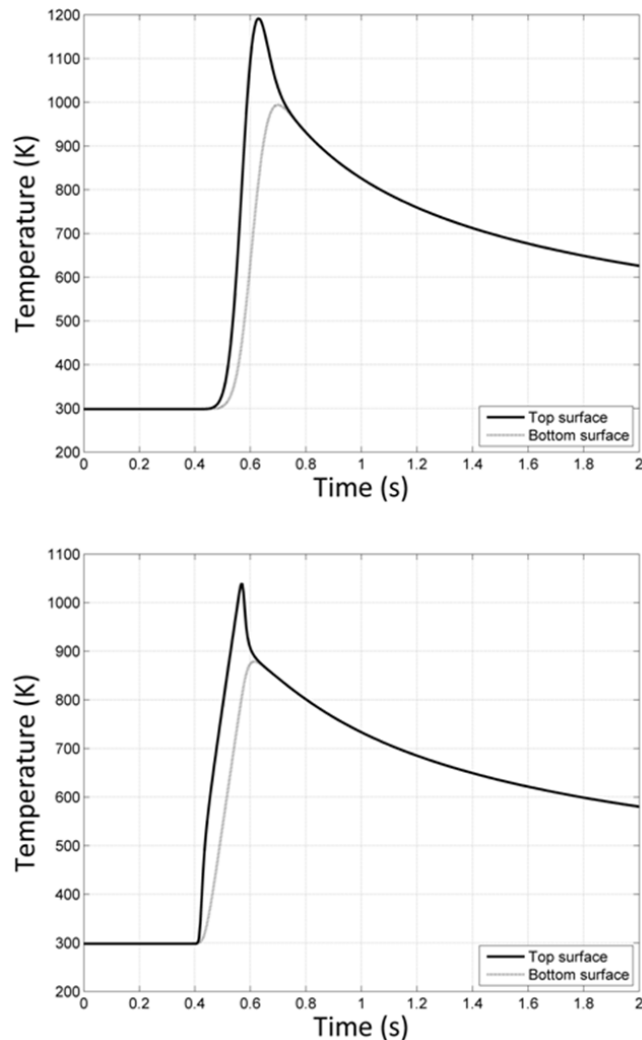


Fig. 6. Simulated temperature profile at the centre point of the sheet on the top and bottom surface for Gaussian intensity distribution (top) and flat top intensity distribution (bottom), 50 x 50 x 1.2 mm DP 1000, 60 mm/s traverse speed, 1800 W average power, 80% absorption.

#### 4. Conclusions

The applicability of the laser forming process for the post-processing and correction of distortion of mechanically formed advanced high strength steel (AHSS) components was investigated numerically and experimentally. A dual phase steel (DP 1000) was bent out of plane using a CO<sub>2</sub> laser, operating in continuous wave mode. Analogous transient thermal finite element (FE) simulations were conducted, the aim of which was to assess the suitability of the laser forming process on the basis of working within metallurgical constraints. As such, chief consideration was

given to the propensity for microstructural change. Results of thermal finite element simulations suggest that austenitization is the main contributing factor to reduction in hardness observed during laser heating, with these transformations limited to the irradiation area due to the selective nature of laser processing. Away from the irradiated area where the laser-induced thermal cycles are less severe, a lesser reduction in hardness may result from the loss of tetragonality in martensitic regions of the dual phase steel.

Regarding optimisation of process parameters to minimise unwanted microstructural transformation, thermal finite element simulations showed that varying process parameter combinations had little effect on the thermal cycle induced in the bulk of the component. Subsequently, it was shown that beam mode could be altered to optimise the thermal cycle in the irradiated region, reducing the peak temperature and therefore offering the potential to reduce the extent of microstructural transformation.

There is significant potential for the application of laser forming bending in the in the post-processing and correction of distortion of mechanically formed AHSS components. The incremental nature of the process makes it suitable for use in closed loop, iterative systems, helping to achieve good manufacturing tolerances. However, the work in this paper has shown that, in order to realise this potential in an industrial environment, process parameters and beam mode must be optimised.

## References

- Edwardson S, Griffiths J, Edwards K, Dearden G, Watkins K. Laser forming: overview of the controlling factors in the temperature gradient mechanism. *Proc Inst Mech Eng Part C* 2010;224(5):1031-1040.
- Griffiths J, Edwardson SP, Boegelein T, Prandina M, Dearden G, Watkins KG. Finite Element Modelling of the Laser Forming of AISI 1010 Steel. *Lasers in Engineering* 2011;22:401-412.
- Griffiths J, Edwardson S, Dearden G, Watkins K. Finite Element modelling of laser forming at macro and micro scales. *Physics Procedia* 2010;5:371-380.
- Vollertsen F, Sakkietitbutra J. Different types to use laser as a forming tool. *Physics Procedia* 2010;5, Part B(0):193-203.
- Neugebauer R, Scheffler S, Poprawe R, Weisheit A. Local laser heat treatment of ultr high strength steels to improve formability. *Prod Eng Res Devel* 2009(- 4-5):- 347-351.
- Bhadeshia HK, Bhadeshia K, Honeycombe R. *Steels: Microstructure and Properties*. 3rd ed.: Butterworth-Heinemann; 2006.
- Smith S, Vrenken J, Van der Veldt T. Structural performance of adhesive and weld bonded joints in AHSS. *Weld World* 2012;57(1):147-156.
- Steen WM, Mazumder J. *Laser Materials Processing*. 6th ed.: Springer; 2010.